

Description of gold and copper anomalies using fractal and stepwise factor analysis according to stream sediments in Lahrud 1:100,000 sheet, NW Iran

Zahra Farahmandfar¹, Mohammadreza Jafari¹, Peyman Afzal^{2*}, Afshin Ashja-Ardalan¹

¹ Department of Geology, North Tehran Branch, Islamic Azad University, Tehran, Iran

² Department of Petroleum and Mining Engineering, South Tehran Branch, Islamic Azad University, Tehran, Iran

*Corresponding author, e-mail: P_Afzal@azad.ac.ir

(received: 01/10/2018 ; accepted: 08/09/2019)

Abstract

This aim of the study is to describe the copper and gold anomalies, by using the combination of the Concentration–Number (C–N) fractal and the stepwise factor analysis, based on stream sediment samples in Lahrud 1:100,000 sheet, NW Iran. The field of study is situated in Alborz–Azerbaijan belt. According to index ore deposit types, elements related to Au and Cu hydrothermal mineralization were selected for this study. Consequently, all the noise elements were removed after applying four steps of factor analysis and As, Sb, Sn, W, Co, Mn, Zn, Ti, Ba, Ni, Cr, Au, Cu, and B were grouped in the five factors. Cu and Au are grouped on factor 4 of the last step (FAC4–4). The C–N log–log plots for factor scores were plotted and threshold values were determined in order to a generation of elemental geochemical maps. The anomalous areas for metallic elements specifically copper and gold, are located in the NW and SW parts of the region which show a correlation between alteration zones, faults, and intrusions.

Keywords: Lahrud, Concentration–Number (C–N) Fractal Model, Stepwise Factor Analysis, Stream Sediments.

Introduction

Geochemical exploration according to stream sediment data has been widely used for different types of ore deposits (Shamseddin–Meygoni *et al.*, 2014; Nazarpour, 2018). Segregate of different geochemical anomalies based on stream sediment data is an important stage to delineate potential areas for mineral exploration (Deng *et al.*, 2010; Pazand *et al.*, 2011; Rantitsch, 2000; Zuo, 2011a; Shamseddin–Meygoni *et al.*, 2014; Afzal *et al.*, 2016; Momeni *et al.*, 2016). Statistical analysis widely applied to separate geochemical anomalies based on different parameters especially mean, median and standard deviation (Arias *et al.*, 2012; Carranza, 2009a, 2010; Davis, 2002; Li *et al.*, 2003; Daneshvar–Saein, 2017). The application of the classical statistical methods are acceptable in a dataset that reveals a normal distribution and consists of independent variables (Asadi *et al.*, 2014). Since the elemental concentration in the crust does not usually follow a normal distribution and also, using traditional methods for finding threshold values can lead to an inaccurate identification of geochemical anomalies (Carranza, 2009a), fractal modeling has been widely utilized in different branches of geosciences and mineral exploration since the 1980s, e.g., Concentration–Area (C–A) by Cheng *et al.*, 1994, Concentration–Distance (C–D) by Li *et al.*, 2003, Concentration–

Volume (C–V) by Afzal *et al.*, 2011 and Concentration Number (C–N) by Hassanpour & Afzal, 2013 which were recommended for geochemical data processing. The aim of this study is to survey geochemical anomalies using a combination of the C–N fractal modeling and the stepwise factor analysis in Lahrud 1:100,000 sheet, NW Iran, according to stream sediments geochemical data.

Geological setting

The NW of Iran is the most complicated region within the Iranian crust. There are numerous and sometimes diverse opinions on its geologic evolution (e.g. Berberian *et al.*, 1981; Majidi, 1981; Sengör, 1990; Alavi, 1991a; Eftekharijad & Asadian, 1992; Golonka, 2004; Kazmin & Tikhonova, 2006; Galoyan *et al.*, 2009; Barzegar & Pourkermani, 2010; Sudi–Ajirlu *et al.*, 2010; Ahmadzadeh & Zamani, 2016). This area was affected by movements of the African and Arabian Plates due to the opening of Atlantic Ocean and the opening the Red Sea, respectively, along with other regions of Iran, Turkey and Caucasus (Fig. 1).

Based on the classification of Iran's structural units, this area is part of the Eocene–age, E–W trending Alborz–Azerbaijan magmatic belt that is related to the western division of the Alborz Cenozoic volcanic belt (Azizi & Moinevaziri, 2009;

Sudi–Ajirli & Jahangiri, 2010). This volcanic belt is separated from the central Iranian plate by the

Tabriz fault to the south and north and extends into Armenia (Azizi & Jahangiri, 2008; Fig. 2).

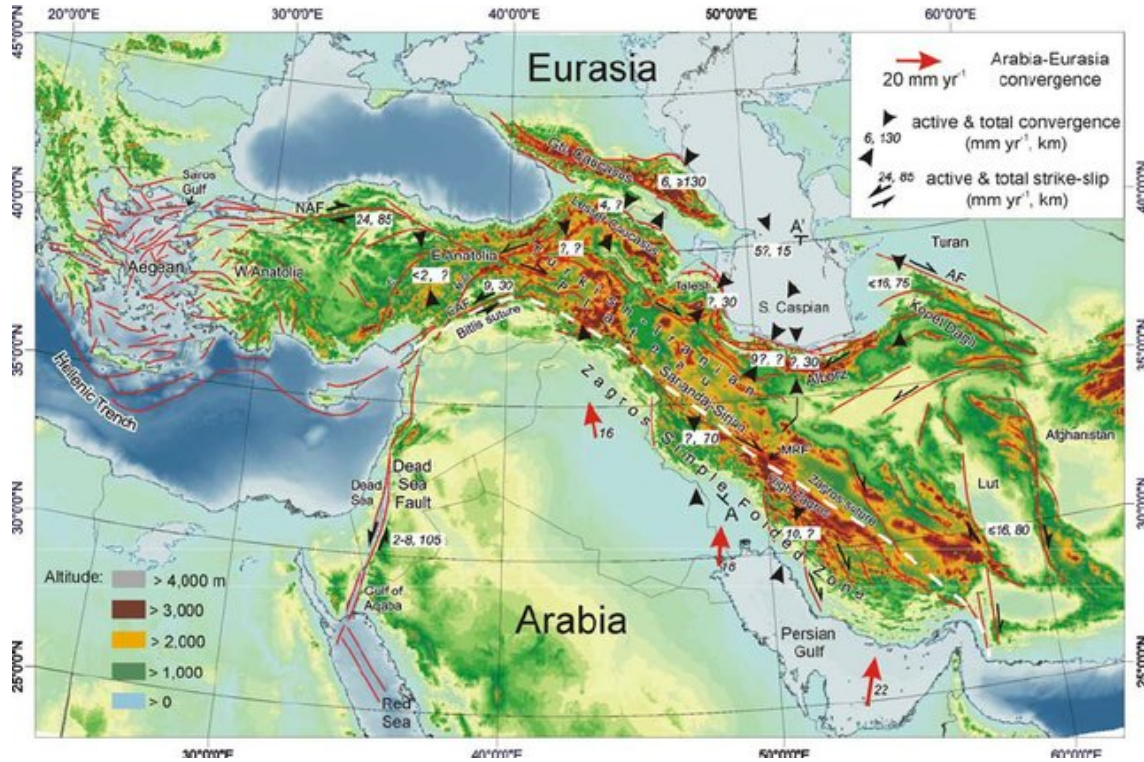


Figure1. Topography and regional structures map of the Arabia– Eurasia collision (after Allen *et al.*, 2003). Situation of Fig. 2 is a black rectangle. Black arrows and numbers in italics are present shortening or slip rate in mm yr⁻¹, followed by finite shortening or strike-slip in kilometers; red arrows present Arabia-Eurasia convergence rates.

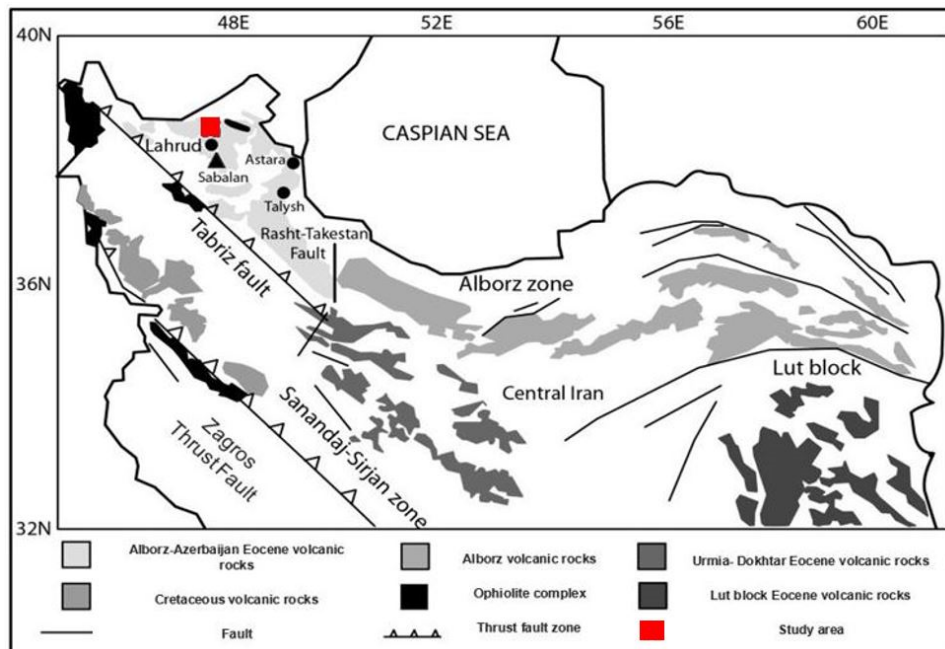


Figure 2. Distribution of Cretaceous and Eocene volcanic rocks and dismembered ophiolites in Iran (after Azizi & Jahangiri, 2008)

Volcanic and plutonic rocks of Eocene and Plio-Quaternary age are widely distributed in this Alborz-Azerbaijan-Lesser Caucasus magmatic belt and are mainly comprise of calc-alkaline to alkaline felsic to mafic volcanic rocks and felsic to intermediate intrusions (Moayyed, 2001; Jamali *et al.*, 2012). The studied area includes alkaline lavas and pyroclastic rocks, associated with sedimentary and volcano-sedimentary units (Ahmadzadeh & Zamani, 2016). The Eocene volcanic mass in the Lahrud region includes volcanic breccias with andesitic, tephritic and trachy-andesitic rock fragments (Fig. 3; Shahbazi-Shiran & Shafaii-Moghadam, 2010). Several small Oligocene sub-volcanic bodies are exposed in the south-western part of the area. Phonotephrite and trachyandesite feeder dykes of the volcanic rocks locally cut volcanic breccias and form parallel sets. The volcanic rocks consists of analcimebearing and analcime-free lavas locally associated with volcanic breccias and pillow lava. Submarine lava eruptions formed widespread volcanic breccias, pillow lavas, and clastic rocks in the early Eocene (Ahmadzadeh & Zamani, 2016). Alunitized, Kaolinitized and Silisified alteration zones occurred in the SW, central and NW parts of the studied region based on remote sensing, field observations and XRD/XRF analysis by several researchers (e.g., Jamali, 2012; Jamali & Mehrabi, 2015). These alteration zones associate with intrusive bodies in the SW part of the Lahrud district. There are two main fault groups with trending of E-W and NW-SE.

Many of epithermal Au deposits of high, medium and low-sulfidation types are located in these faults and related structures (Jamali, 2012; Jamali & Mehrabi, 2015).

Arasbaran belt is situated in this sheet and hosts many Cu-Au porphyry and epithermal mineralization. There are a Cenozoic volcano-plutonic assemblage with few sediments in the upper part, and Cenozoic clastic deposits of Para-Tethys basin in the north of the Lahrud region. In addition, small ophiolitic complexes sporadically crop out north of the Arasbaran belt (e.g., north of Lahrud; Jamali & Mehrabi, 2015).

Cu and Au are main mineralized elements in these studied area in form of deposits, occurrences. Porphyry and epithermal deposits are abundant in this region. Based on this reasons, Cu and Au were selected as target elements.

Methods

Statistical analysis

Multivariate statistical analysis especially factor analysis is a suitable approach to classify and reduce the number of geochemical variables (Muller *et al.*, 2008; Yousefi *et al.*, 2012; Zuo *et al.*, 2009; Zuo, 2011a, b). This technique is used for the finding of paragenesis of target elements. The stepwise factor analysis is a developed multivariate method for reducing noise elements and determining elemental paragenesis for a regional scale of mineral exploration (Yousefi *et al.*, 2012; Afzal *et al.*, 2016, 2017).

Fractal modeling

One of the essential operations for mineral exploration is a determination of background/host rock and related geochemical anomalies/mineralized zones (Cheng *et al.*, 1994; Afzal *et al.*, 2011; Jebeli *et al.*, 2018). The fractal/multifractal models which is considered to be a widely applied instrument in different branches of geosciences, was proposed by Mandelbrot, 1983. Various changes in the fundamental behavior of phenomenon can be defined by different fractal dimensions (Li *et al.*, 2003; Carranza, 2009a,b; Afzal *et al.*, 2016, 2017; Zuo *et al.*, 2009, 2016; Hassanpour & Afzal, 2013; Daneshvar Saein, 2017; Jebeli *et al.*, 2018; Soltani, 2019; Zamyad, 2019; Afzal, 2019; Mirzaei, 2020; Alipour Shahsavari, 2020). Several fractal models are widely used in geosciences including Concentration-Area (C-A; Cheng *et al.*, 1994), Concentration-Perimeter (C-P; Cheng, 1995), Concentration-Distance (C-D; Li *et al.*, 2003), Concentration-Volume (C-V; Afzal *et al.*, 2011) and Concentration-Number (C-N; Hassanpour & Afzal, 2013). The C-N (Concentration-Number) fractal model, proposed by Hassanpour & Afzal, 2013, for various anomalies and background separation, can be described as follows:

$$N(\geq\beta) \propto \beta^{-\gamma} \quad (1)$$

where $N(\geq\beta)$ is the number of the quantity (such as Cu grade in this scenario) greater than the β value, which is the value of the concentration of study element, and γ is a fractal dimension. The value must not endure any pretreatment, and results can be shown as a C-N log-log plot. This log-log plot represents grade distribution and the relationship between different mineralized zones. It can be correlated with geological characteristics of ore deposit for different purposes, same as a pre-step for grade and geological modeling and estimation (Deng *et al.*, 2010; Sadeghi *et al.*, 2012; Hassanpour & Afzal, 2013; Afzal *et al.*, 2016, 2019).

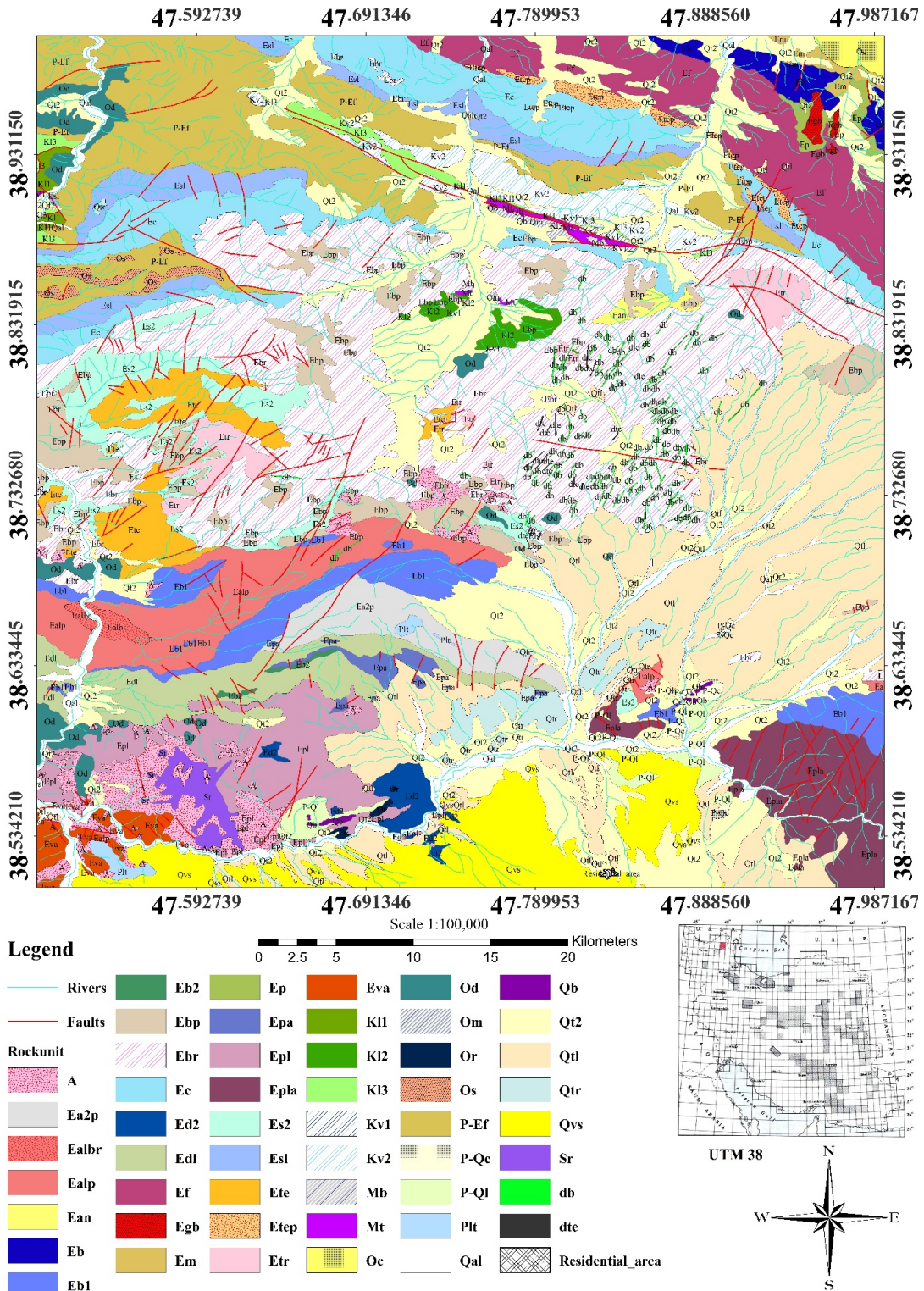


Figure 3. Geological map of Lahrud region (modified after Babakhani & Nazer, 1989) (*db*: Andesite, Andesitebasaltic dyke; *d^{te}*: Analcimetephrite, Phenolitic dyke; *A*: Alunitized and Kaolinitized zone; *O^r*: Nepheline syenite, Phenolite; *O^d*: Granodiorite, Quartzdioritic subvolcanic bodies; *O^c*: Polygenic conglomerate; *E^m*: Alternation of thin bedded marl and sandstone; *E^b*: Olivine basalt; *E^{gb}*: Olivinegabbro; *E^p*: Megaporphyrlatite; *E^f*: alternation of shale, sandstone, marl, conglomerate; *E^{tep}*: Tephritic pillow lavas; *E^{pla}*: Megaporphyritic latite and Andesitic lava flows; *E^{d2}*: Dacite, Ignemberite; *E^{va}*: Andesite, Latiteandesite; *E^{pl}*: Porphyritic latite lava

flows; E^{b3} : Olivinebasalt, Basanite; E^{dl} : Dacite, Ignemberite, Trachyandesite; E^{b2} : Andesitebasalt, Basanite; E^{pa} : Megaporphyritic andesite and Andesitebasalt lava flow; E^{a2p} : Trachyandesite porphyry; E^{bl} : Pyroxene Andesite, Andesitebasalt; E^{alp} : Andesite porphyry; E^{albr} : Submarine volcanic breccia Hyaloclastite; E^{te} : Porphyritic Analcime Tephrite, Analcimite; E^{s2} : Sandstone, marl, conglomerate, breccia; E^r : Trachyte, trachyandesite; E^{bp} : Andesitic and tephritic pillow lavas; E^{tm} : Tephritic breccia; E^{br} : Volcanic breccia with pyroxene Andesite, tephritic and Trachyandesitic fragments; E^c : Thick bedded tuffaceous sandstone, conglomerate, breccia; E^{tl} : Tin bedded tuffaceous sandstone, microconglomerate; $P-E^f$: Alternation of thin bedded sandstone, shale, sandylimestone (Flyschoid); K^{v2} : Andesite and Trachyandesitic lava flows with some pillow structures; K^{l3} : Alternation of crystalized cherty limestone and thin bedded marly and sandy limestone; K^{l2} : Thin bedded marly and sandy limestone; K^{v1} : submarine volcanics (Andesite, Hyaloclastite); K^{l1} : red brown Pelagic limestone; O^m : Ophiolitic mélange: imbricated pridotite, gabbro, diabase, schist, gneiss, marble, plagiogranite; S^r : Serpentinite, listvenite; M^b : Marble; M^r : Sericite, Muscovite schist, chlorite Epidote schist, Quartzite, metadiabase; Q^{al} : Recent Alluviums; Q^{t2} : Young terraces and fans; Q^{tr} : Travertine; Q^{vs} : Sabalan volcanosediments, mainly Tuff, Ash, Lahar, Conglomerate; Q^{ol} : old terraces, Clay, Sand, Silt, locally Gypsum and Conglomerate; Q^b : Basalt, Andesite basalt; $P-Q^l$: Ignemberite, Pelean Breccia; $P-Q^c$: Unconsolidated Volcanogenic Conglomerate; P^d : Trachytic and dacitic domes; O^r : Rhyolite Rhyodacite.

The C–N fractal model shows that there is a relationship between elemental concentrations and their sample cumulative number based on the concentration in a survey area. In this model, a power–law frequency model has been used to interpret Number–Concentration relation based on elemental concentration frequency distribution and the cumulative number of samples (Li *et al.*, 1994; Sanderson *et al.*, 1994; Shi & Wang, 1998; Turcotte, 1997; Wang *et al.*, 2008; Zuo *et al.*, 2009).

Stepwise factor analysis

Geochemical data often shows compositional characteristics and represents a closed number system, therefore, a data transformation is crucial to reveal their inter–element relationships prior to analysis (Buccianti & Grunsky, 2014; Carranza, 2009a, 2011; Filzmoser *et al.*, 2009a; Yousefi *et al.*, 2012; Zuo, 2014; Zuo *et al.*, 2013a, b). The geochemical data is inherently multivariate, which means that anomalies are expressed in more than one element (Asadi *et al.*, 2014). Factor analysis is one of the most popular multivariate analyses which is demonstrated as a powerful tool to visualize high–dimensional data in lower–dimensional spaces based on variance and covariance matrix (Rezaei *et al.*, 2015). It is a practical tool for combining several correlated variables into a single variable and therefore for reducing the dimensionality of datasets into uncorrelated principal components based on covariance or correlations of variables which represents the interrelationships among the multi–dimensional variables (Jolliffe, 2002;

Reimann *et al.*, 2005; Zuo, 2011a). Using this method, a large set of geochemical variables are combined in to a few factors. (Shamseddin–Meygani *et al.*, 2014). Consequently, the results by classical factor analysis become unreliable if outliers are present in the data (Filzmoser & Todorov, 2011). Thus, the rotated eigenvectors may be greater resemblance (with less variance) to actual physical states than the un–rotated eigenvectors (Shamseddin–Meygooni *et al.*, 2014).

Discussion

Dataset

In this study, about 600 stream sediment samples were collected in Lahrud region by the Geological Survey and Mineral Exploration of Iran in 2003 (Fig. 4). These samples were analyzed using the Induced Coupled Plasma–Mass Spectroscopy (ICP–MS) analytical method. Stream sediments samples extended beyond the Lahrud to identify mineralization of precious metals especially Au and Cu. Statistical parameters of these elements (Au and Cu) calculated contain average, median, mode, maximum and minimum values, variance, standard deviation, skewness, and kurtosis (Table 1). Elemental histograms show that there are not normal distribution (Fig. 5). In this condition, elemental anomalies commence from their median based on statistical methods. According to this position, Au and Cu anomalies are beginning from 2 ppb and 72 ppm (Table 1). Geochemical maps were generated by ArcGIS 10.4.1 and Rockworks 15 softwares.

Table 1. The statistical parameters of the gold and copper on Lahrud stream sediment samples

	Average	Median	Mode	Max.	Min.	STDEV	Var.	SKEW	KURT
Au (ppb)	2.49491	2	2	40	0.75	2.90497	8.43885	7.24479	73.48562
Cu (ppm)	74.0834	72.3500	101	392.0000	14.5000	25.95602	673.71547	3.33016	37.63476

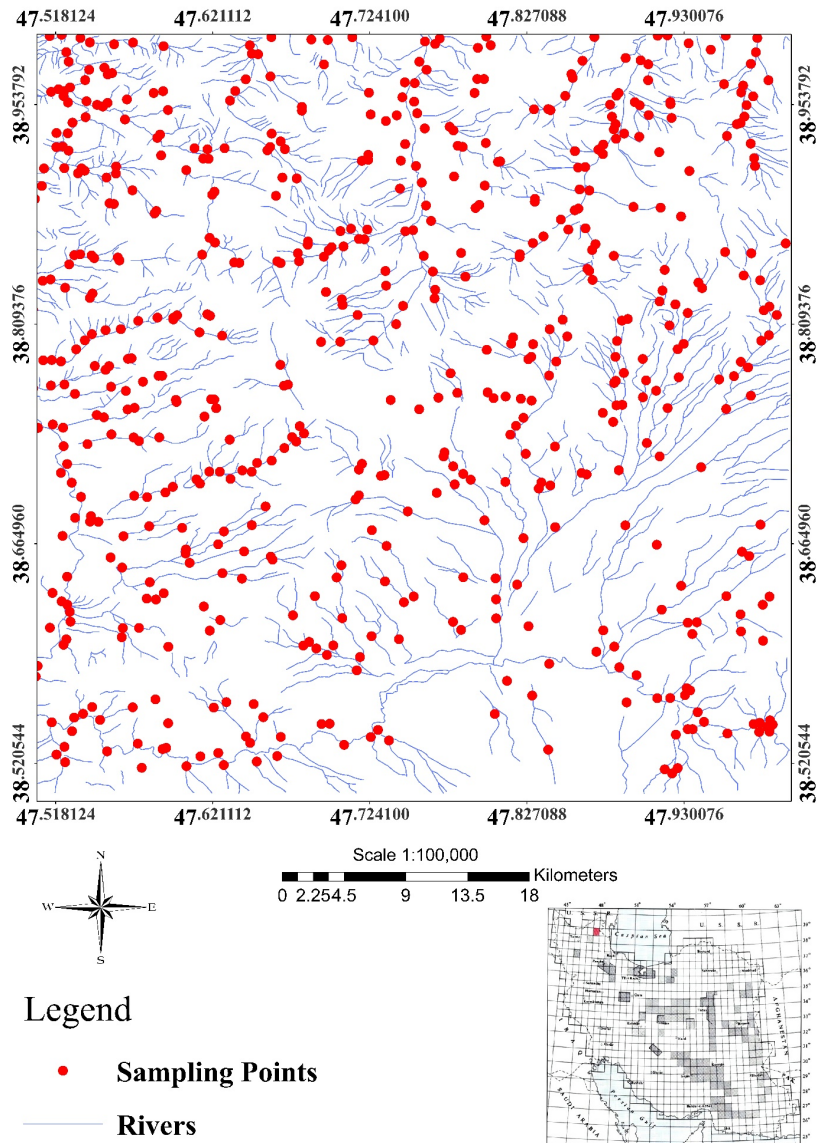


Figure 4. Stream sediment samples map of Lahrud 1:100,000 sheet.

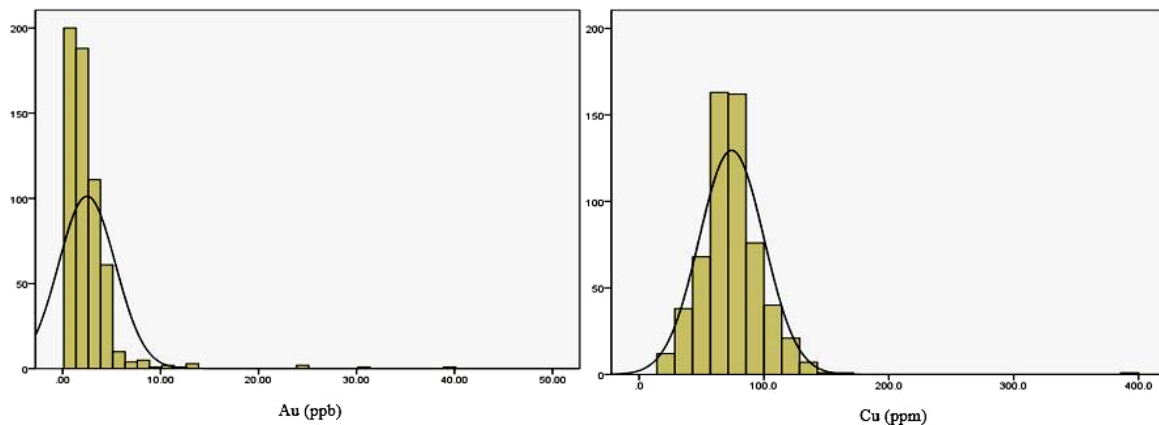


Figure 5. Gold and copper histograms of Lahrud stream sediment.

Application of fractal and factor analysis

These stream sediment data were transformed by an Ln transformation for factor analysis. For reduction of dimensionality, factor analysis was performed in stream sediments geochemical data. Results were obtained by the stepwise factor analysis which was carried out using stream sediment data. The factor analysis was applied, and 22 elements were classified using SPSS software to the following groups; For a better illustration of the extracted factors, the factor plot in rotated space is illustrated in Fig. 6. The factor analysis was applied to the five steps of the Lahrud stream sediments geochemical data. The stepwise factor analysis was carried out by removing noisy elements which were not located in any factors. These elements were removed and also factors were cleaned. On the other hand, score

of the noisy elements are lower than 0.6. At the first, second and third steps Mo, Be, Hg; Pb, Ag, Sr; Se, Bi were removed, respectively. At the final step As, Sb, Sn, W, Co, Mn, Zn, Ti, Ba, Ni, Cr, Au, Cu and, B remained and Au and Cu were chosen as the main target (Tables 2; Fig. 6). Finally, Cu and Au were grouped in factor 4 from fourth step (FAC4–4) as depicted in Table 2 and Fig. 7. For a better illustration of the extracted factors, the factor plot in rotated space is illustrated in Fig.6.

Based on C–N log–log plots of the elements, there are four geochemical populations for Au (Fig.8) and Cu (Fig.9). The straight fitted lines were obtained based on least–square regression (Agterberg *et al.*, 1996; Spalla *et al.*, 2010; Yasrebi & Hezarkhani, 2019).

Table 2. The final step of factor analysis of Lahrud stream sediment elements. Bold values indicate existing elements in each factor (Based on absolute threshold of 0.6).

Element	Component				
	1	2	3	4	5
Au	.137	-.111	-.015	.779	-.031
Co	-.396	.696	.478	.113	.025
Cu	-.164	.138	-.038	.756	-.018
Mn	-.390	.743	-.202	.205	-.023
Zn	.094	.918	-.138	.037	-.050
Ba	-.073	.094	-.646	.158	.096
Ti	.069	.820	.356	-.156	-.020
As	.748	-.208	-.271	.122	-.268
B	.017	-.073	-.028	-.039	.963
Sb	.899	-.152	-.151	.020	.009
Sn	.713	.338	.050	-.136	.230
W	.833	-.085	-.111	-.033	.015
Ni	-.288	.026	.844	.100	.049
Cr	-.206	.190	.889	.008	.058

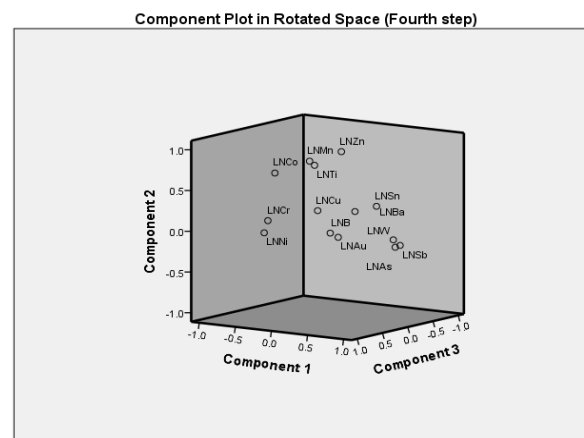


Figure 6. Component plot in rotated space in final stage of stepwise factor analysis.

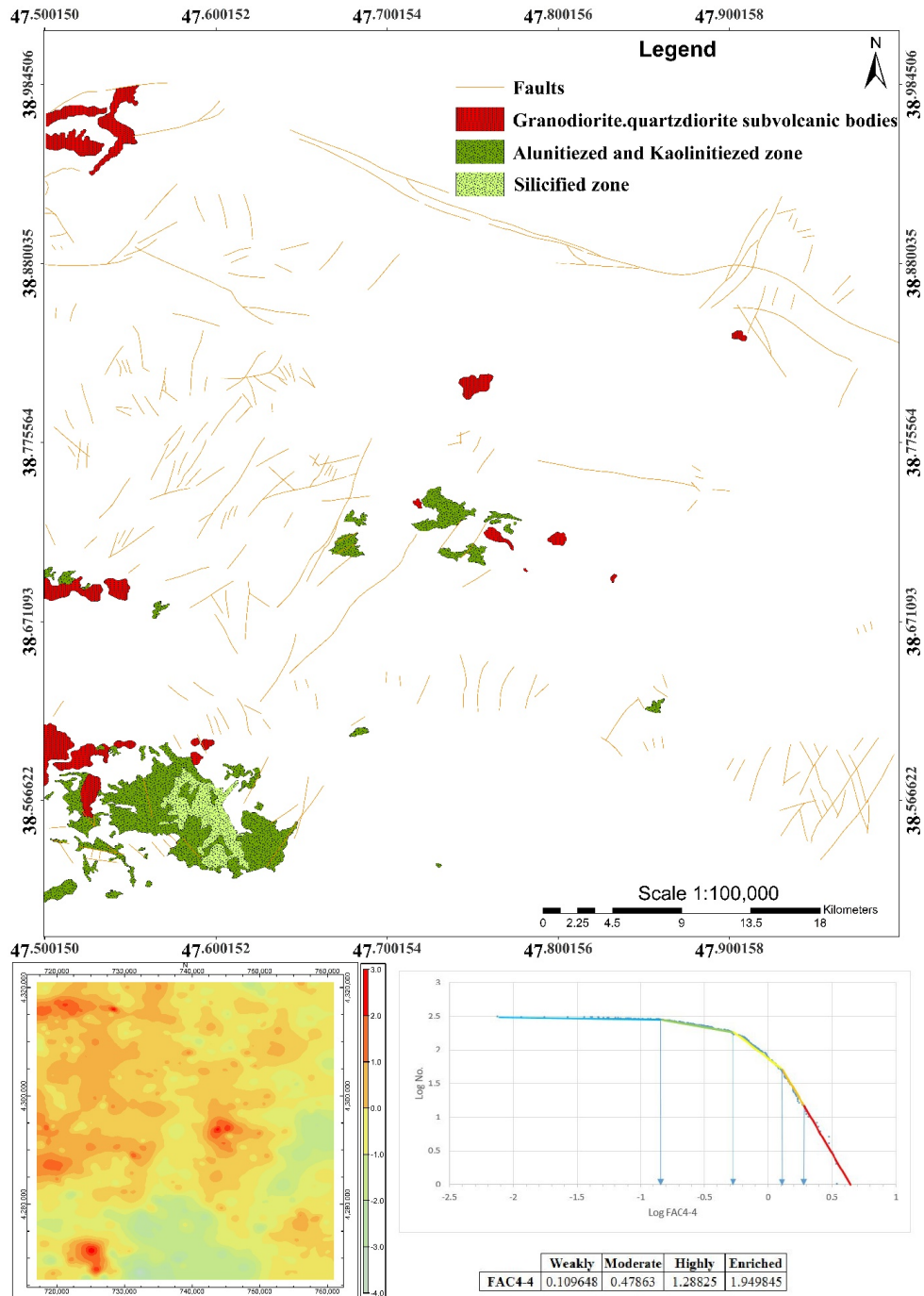


Figure 7. Hydrothermal alterations, intrusions and FAC 4-4 geochemical anomaly map.

Extreme anomalies of Au and Cu start from 24 ppb and 240 ppm, respectively. In addition, C-N log plot of the fourth factor was generated and five line segments were fitted for this factor (Fig.7).

Main anomalous parts of Au and Cu were located in the SW and NW, respectively (Fig 8 and Fig.9) and FAC 4-4 was found in the SW, NW and

Central of the area. The main parts of Au anomalous areas have conformed to the SW alteration zones (Alunitized, Kaolinitized and Silicified zones) and intrusive rocks (Fig. 8); Cu anomalies are located in the NW of area follow the intrusive rocks (Fig.9).

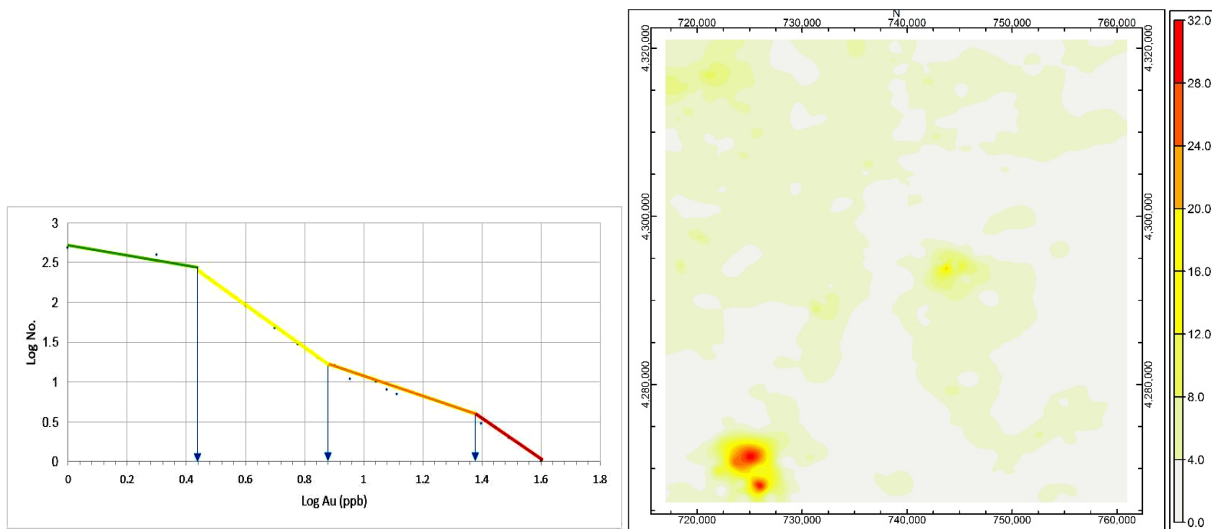


Figure 8. C-N log-log plot and geochemical anomaly map of Au.

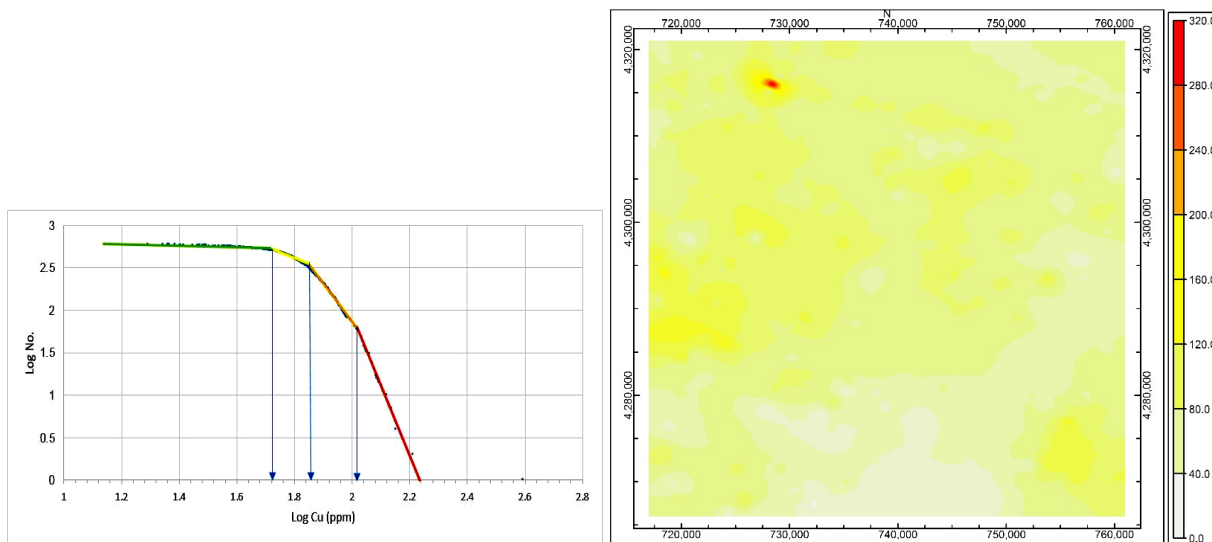


Figure 9. C-N log-log plot and geochemical anomaly map of Cu.

Factor 4–4 (Cu and Au) map show main anomalies in red colored (More than 2) which are located in the NW, SW, western and central parts of the Lahrud region based on factor scores. Factor scores between 0 and -1 are shown weakly anomalies as depicted with yellow color in the Fig. 7. FAC 4–4 anomalous areas located in the NW, SW, and Central parts of Lahrud sheet conformed to alteration zones (Alunitized and Kaolinitized zones) and intrusive rocks, notable (Fig.7). The anomalies are associated with intrusive rocks and alteration zones also have a relationship with the faults system of the sheet (Fig.7). Lahrud faults mechanism appeared to have caused the outcrop of the intrusions and rise hydrothermal alterations on

the surface that caused the surrounding rocks to be altered. The main faults trend involved are the SW–NE (Fig. 7). The significant point is the main mineralization which conforms to alterations and intrusive masses. In this region, hydrothermal alterations on SW and Central and intrusions in the SW, Central and NW; Au and Cu geochemical anomalies follow those trends. As seen in figure 7 which indicates a close connection between those.

Au and Cu were selected as a main target and the C–N fractal model was also performed on the final stepwise factor analysis and showed high intensity threshold for gold and copper (Table 3 and Fig.8 and Fig.9). Anomalies of other related elements including Ag, As, Mo, Pb and Sb were separated

based on C–N log–log plots (Fig. 10). Their anomalies were mapped based on the C–N fractal modeling, as depicted in Fig. 11. Their main anomalies were situated in the SW part of the studied region. It can be represented that there is main target for exploration of epithermal and porphyry deposits.

Table 3. Thresholds of Au and Cu in Lahrud sheet based on C–N fractal model.

	Low intensity threshold	Moderate intensity threshold	High intensity threshold
Au	2.75423	7.58578	23.9883
Cu	4.7088	63.0957	104.713

Conclusion

In the present study, the fractal modeling was utilized to outline Cu and Au stream sediment elements anomalies in Lahrud area, NW Iran. The results obtained by the combined model show that geochemical anomalies. The achieved anomalies have sharp and considerable correlation with evidence of silicified alteration, argillic zones (Alunite and Kaolinite) and granodiorite and quartz–diorite subvolcanic bodies. In addition, the fractal model can be a useful method for geochemical exploration.

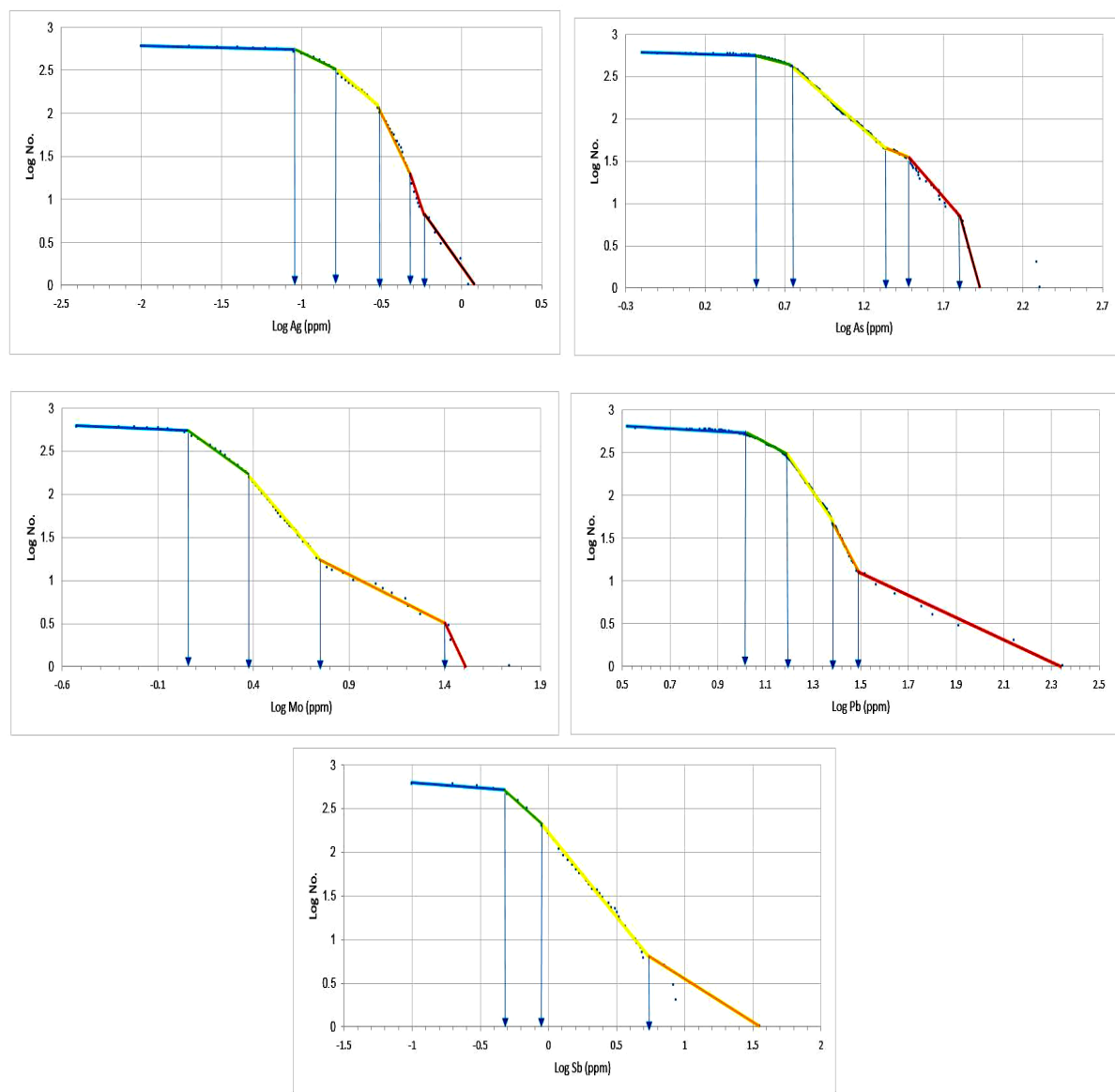


Figure 10. C–N log–log plots for Ag, As, Mo, Pb and, Sb.

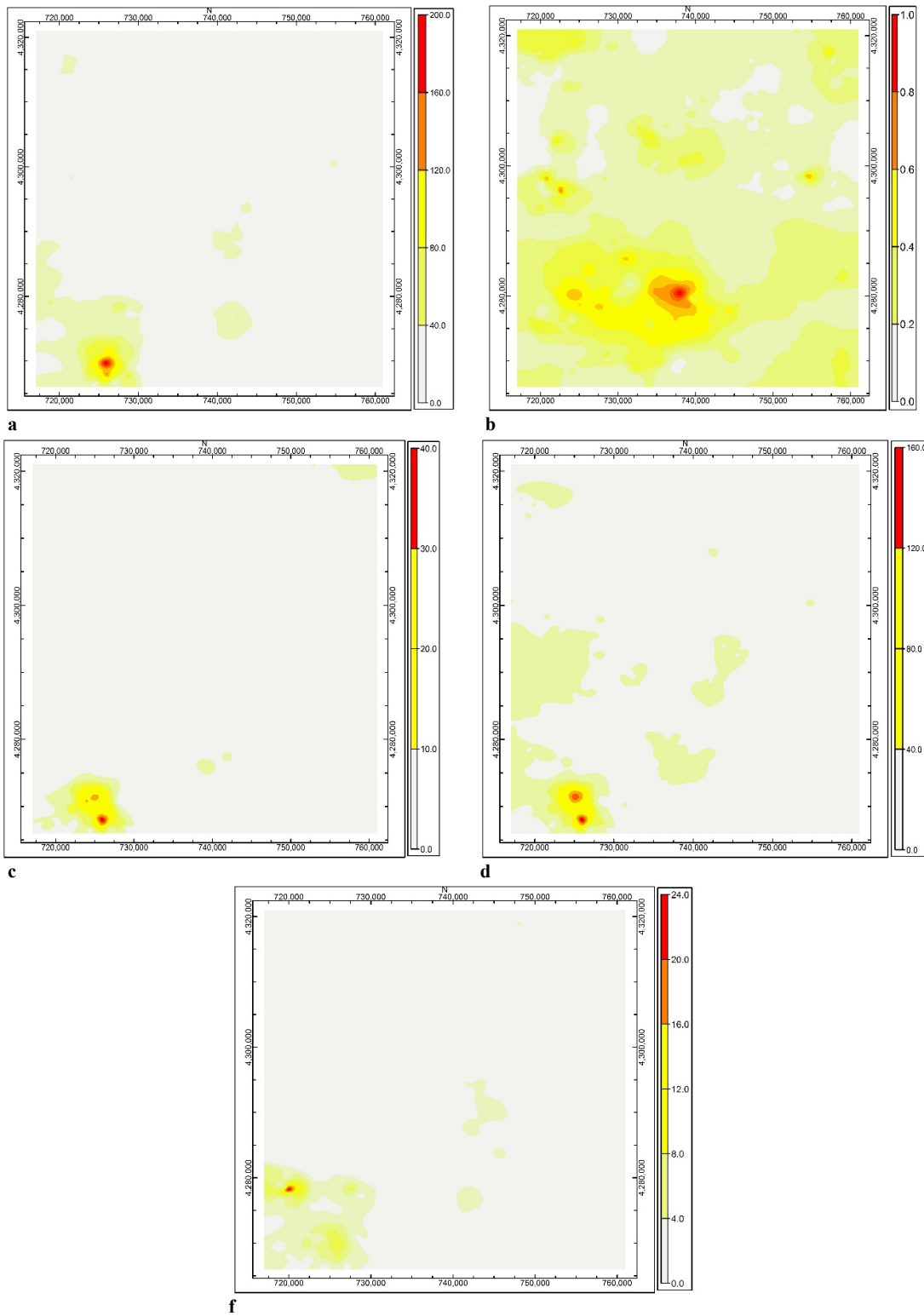


Figure 11. Geochemical maps for As (a), Ag (b), Mo (c), Pb (d) and, Sb (f) based on the C-N fractal model.

The advantages of this method rely essentially on its accuracy due to removing noises from

geochemical data. The result obtained by the model due to indicate that Au and Cu highly anomalies in

SW and NW, respectively. As well as, gold and copper geochemical anomalies and relevant factor (FAC 4–4) confirm the alteration zones and intrusions which is in line with the process of most

fault trends in this region. The combination of intrusion bodies, alteration zones, and Au, Cu potential maps are remarkable.

References

- Agterberg, F.P., Cheng, Q., Brown, A., Good, D., 1996. Multifractal modeling of fractures in the Lac du Bonnet Batholith, Manitoba. *Computers and Geosciences* 22, 497–507.
- Afzal, P., Yousefi, M., Mirzaei, M., Ghadiri-Sufi, E., Ghasemzadeh, S., Daneshvar Saein, L., 2019. Delineation of podiform-type chromite mineralization using Geochemical Mineralization Prospectivity Index (GMPI) and staged factor analysis in Balvard area (southern Iran). *Journal of Mining and Environment* 10: 705–715.
- Afzal, P., Ahmadi, K., Rahbar, K., 2017. Application of fractal-wavelet analysis for separation of Geochemical anomalies. *Journal of African Earth Sciences*, 128:27–36.
- Afzal, P., Eskandarnejad Tehrani, M., Ghaderi, M., Hosseini, M.R., 2016. Delineation of supergene enrichment, hypogene and oxidation zones utilizing staged factor analysis and fractal modeling in Takht-e-Gonbad porphyry deposit, SE Iran. *Journal of Geochemical Exploration*, 161:119–127.
- Afzal, A., Fadarar, Y., Khakzad, A., Moarefvand, P., Rashidnejad, N., 2011. Geochemical anomaly separation by multifractal modeling in Kahang (Gor Gor) porphyry system, Central Iran. *Journal of Geochemical Exploration*, 108:220–232.
- Ahmadzadeh, Gh.R., Zamani, R., 2016. A study of different zoning types in clinopyroxenes of sodic and potassic alkaline volcanic rocks from North Lahrud, NW Iran. *Iranian Journal of Earth Sciences*, 8: 25–35.
- Alavi, M., 1991a. Sedimentary and structural characteristics of the Paleo-Tethys remnants in northeastern Iran. *Geological Society of American Bulletin*, 103: 983–992.
- Alavi, M., 1991b. Tectonic Map of Middle East in scale 1:5000000. Geological Survey of Iran, Tehran.
- Alipour Shahsavari, M., Afzal, P., Hekmatnejad, A., 2020. Identification of geochemical anomalies using fractal and LOLIMOT neuro-fuzzy modeling in Mial area, Central Iran. *Journal of Mining and Environment* 11: 99–117.
- Arias, M., Gumiel, P., Martín-Izard, C., 2012. Multifractal analysis of geochemical anomalies: a tool for assessing prospectivity at the SE border of the Ossa Morena Zone, Variscan Massif (Spain). *Journal of Geochemical Exploration*, 122: 101–112.
- Asadi, H.H., Kianpouryan, S., Lu, Y.J., McCuaing, T.C., 2014. Exploratory data analysis and C–A fractal model applied in mapping multi-element soil anomalies for drilling: A case study from the Sari Gunay epithermal gold deposit, NW Iran. *Journal of Geochemical Exploration* 145: 233–241.
- Azizi H., Jahangiri, A., 2008. Cretaceous subduction-related volcanism in the northern Sanandaj–Sirjan Zone, Iran. *Journal of Geodynamics* 45: 178–190.
- Azizi H., Moinevaziri, H., 2009. Review of the tectonic setting of Cretaceous to Quaternary volcanism in northwestern Iran. *Journal of Geodynamics* 47: 167–179.
- Barzegar, A., Pourkermani, M., 2010. Structural evolution of folded zone of Allahyarlu in western Alborz. 21st Congress of Geological Sciences and 15th Congress of Geological Survey of Iran, Urmia University (In Persian).
- Berberian, M., Babakhani, A., Amidi, S.M., 1981. Discovery of southern continuation of Sevan–Akera ophiolitic belt in northwestern Iran. Internal report of the Geological Survey, 12 pp. (In Persian).
- Buccianti, A., Grunsky, E., 2014. Compositional data analysis in geochemistry: are we sure to see what really occurs during natural processes. *Journal of Geochemical Exploration*, 141: 1–5.
- Carranza, E J M., Sadeghi, M., 2010. Predictive mapping of prospectivity and quantitative estimation of undiscovered VMS deposits in Skellefte district (Sweden). *Ore Geology Reviews*, 38(3): 219–241.
- Carranza, E.J.M., 2009a. Geochemical anomaly and mineral prospectivity mapping in GIS. *Handbook of Exploration and Environmental Geochemistry*, 11. Elsevier, 351 pp.
- Carranza, E.J.M., 2009b. Controls on mineral deposit occurrence inferred from analysis of their spatial pattern and spatial association with geological features. *Ore Geology Reviews*, 35: 383–400.
- Carranza, E.J.M., 2011. Analysis and mapping of geochemical anomalies using logratio transformed stream sediment data with censored values. *Journal of Geochemical Exploration*, 110: 167–185.
- Cheng, Q., 1995. The perimeter–area fractal model and its application to geology. *Journal of Mathematical Geology*, 27: 69–82.
- Cheng, Q., Agterberg, F.P., Ballantyne, S.B., 1994. The separation of geochemical anomalies from background by fractal methods *Journal of Geochemical Exploration*, 51: 109–130.
- Daneshvar Saein, L., 2017. Delineation of enriched zones of Mo, Cu and Re by concentration–volume fractal model in Nowchun Mo–Cu porphyry deposit, SE Iran. *Iranian Journal of Earth Sciences*, 9: 64–72.
- Davis, J.C., 2002, *Statistics and data analysis in Geology* (3rd ed.), John Wiley & Sons Inc., New York, p.p. 342–353.

- Deng, J., Wang, Q., Yang, L., Wang, Y., Gong, Q., Liu, H., 2010. Delineation and explanation of geochemical anomalies using fractal models in the Heqing area, Yunnan Province, China. *Journal of Geochemical Exploration*, 105 (3): 95–105.
- Eftekharnjad, J., Asadian, A., 1992. Age of metamorphic and ophiolitic complex of Asalem–Shanderman and its geodynamic relation with Paleotethys and Caspian oceanic lithosphere. *Journal of Earth Sciences, Geological Survey of Iran*, No. 3 (In Persian).
- Filzmoser P., Todorov V., 2011. Review of robust multivariate statistical methods in high dimension. *Analytical Chemical Acta* 705: 2–14.
- Filzmoser, P., Hron, K., Reimann, C., 2009a. Principal components analysis for compositional data with outliers. *Environmetrics* 20: 621–632.
- Galoyan, G., Rolland, Y., Sosson, M., Corsini, M., Billo, S., Verati, C., Melkonyan, R., 2009. Geochemistry and $^{40}\text{Ar}/^{39}\text{Ar}$ dating of Sevan Ophiolites, Lesser Caucasus, Armenia): Evidences for Jurassic Back–arc opening and hot spot event between the South Armenian Block and Eurasia. *Journal of Asian Earth Sciences*, 34:135–153.
- Golonka, J., 2004. Plate tectonic evolution of the southern margin of Eurasia in the Mesozoic and Cenozoic. *Tectonophysics*, 381: 235–273.
- Hassanpour, S., Afzal, P., 2013. Application of concentration–number (C–N) multifractal modeling for geochemical anomaly separation in Haftcheshmeh porphyry system, NW Iran. *Arabian Journal of Geosciences*, 6(3):957–970.
- Jamali, H., 2012. Metallogenic Zonation and Their Tectono–magmatic Control in Ahar–Arasbaran Magmatic Belt, NW Iran (PhD Thesis) Kharazmi University, Tehran, 372 pp. (in Persian with English abstract).
- Jamali, H., Mehrabi, B., 2015. Relationships between arc maturity and Cu–Mo–Au porphyry and related epithermal mineralization at the Cenozoic Arasbaran magmatic belt. *Ore Geology Reviews* 65: 487–501.
- Jamali H., Yaghubpur A., Mehrabi B., Dilek Y., Daliran F., Meshkani A., 2012. Petrogenesis and Tectono–Magmatic Setting of Meso–Cenozoic Magmatism in Azerbaijan Province, Northwestern Iran. *Petrology New Perspectives and Applications*. In Tech China.
- Jebeli, M., Afzal, P., Pourkermani, M., Jafarirad, A.R., 2018. Correlation between rock types and copper mineralization using fractal modeling in Kushk–e–Bahram deposit, Central Iran. *Geopersia Journal* 8 (1): 131–141.
- Jolliffe T., 2002. *Principal component analysis*, 2nd edn. Springer, New York, 1–487.
- Kazmin, V.G., Tikhonova, N.F., 2006. Late Cretaceous–Eocene Marginal Seas in the Black Sea Caspian Region: Paleotectonic Reconstructions. *Geotectonics*, 40(3): 169–182.
- Li, C., Ma, T., Shi, J., 2003. Application of a fractal method relating concentrations and distances for separation of geochemical anomalies from background. *Journal of Geochemical Exploration*, 77: 167–175.
- Li, C., Xu, Y., Jiang, X., 1994. The fractal model of mineral deposits. *Journal of Geology Zhejiang*, 10: 25–32.
- Majidi, B., 1981. The ultrabasic lava flows of Mashhad, North East Iran. *Geological Magazine*, 118(1): 49–58.
- Mandelbrot, B.B., 1983. *The fractal geometry of nature*. Freeman, San Fransisco. mineralized zones in the Zaghia iron ore deposit, Central Iran. *Journal of Geochemical Exploration*, 122: 9–19.
- Mirzaei, M., Afzal, P., Adib, A., Rahimi, E., Mohammadi, Gh., 2020. Detection of zones based on ore and gangue using fractal and multivariate analysis in Chah Gaz iron ore deposit, Central Iran. *Journal of Mining and Environment* (In press).
- Moayyed M., 2001. Investigation of Tertiary volcano–plutonic bodies in west Alborz–Azarbayejan (Hashtjin area). Ph.D Thesis in Shahid Beheshti University, Iran (in Persian).
- Momeni, S., Shahrokhi S.V., Afzal, P., Sadeghi, B., Farhadinejad, T., Nikzad, M.R., 2016. Delineation of the Cr mineralization based on the stream sediment data utilizing fractal modeling and factor analysis in the Khoy 1:100,000 sheet, NW Iran. *Journal of Bulletin of the Mineral Research and Exploration*, 152: 143–151.
- Muller J., Kylander, M., Martinez–Cortizas, A., Wüst, R.A.J., Weiss, D., Blake, K., Coles, B., Garcia–Sanchez, R., 2008. The use of principle component analyses in characterizing trace and major elemental distribution in a 55 kyr peat deposit in tropical Australia: implications to paleoclimate. *Journal of Geochemistry Cosmochemistry Acta* 72: 449–463.
- Nazarpour, A., 2018. Application of C–A fractal model and exploratory data analysis (EDA) to delineate geochemical anomalies in the: Takab 1:25,000 geochemical sheet, NW Iran. *Iranian Journal of Earth Sciences*, 10: 173–180.
- Pazand, K., Hezarkhani, A., Ataei, M., Ghanbari, Y., 2011. Application of multifractal modeling technique in systematic geochemical stream sediment survey to identify copper anomalies: a case study from Ahar, Azarbaijan, Northwest Iran. *Journal of Chemie der Erde Chemistry*, 71: 397–402.
- Rantitsch, G., 2000. Application of fuzzy clusters to quantify lithological background concentrations in stream–sediment geochemistry. *Journal of Geochemical Exploration*, 71: 73–82.
- Reimann, C., Garrett, R.G., 2005. Geochemical background–concept and reality. *Sci. Total Environ.* 350 (1–3): 12–27.
- Rezaei, S., Lotfi, M., Afzal, P., Jafari, M.R., Shamseddin Meigoony, M., 2015. Delineation of Cu prospect utilizing multifractal modeling and stepwise factor analysis in Noubaran 1:100,000 sheet, Central of Iran. *Arabian Journal of Geosciences*, 8: 7343–7357.

- Sadeghi, B., Moarefvand, P., Afzal, P., Yasrebi, A.B., Saein, L.D., 2012. Application of fractal models to outline mineralized zones in the Zaghia iron ore deposit, Central Iran. *Journal of Geochemical Exploration*, 122: 9–19.
- Sanderson, D.J., Roberts, S., Gumiel, P., 1994. A fractal relationship between vein thickness and gold grade in drill core from La Codosera, Spain. *Economic Geology*, 89: 168–173.
- Sengör, A.M.C., 1990. Plate tectonics and orogenic research after 25 years: A Tethyan perspective. *Earth–Science Reviews*, 27: 1–201.
- Shahbazi–Shiran, H., Shafaii–Moghadam, h., 2010. Geochemistry and petrogenesis of Paleocene–Eocene shoshonitic lavas in Lahrud region, NW of Iran. 6th Symposium of the International Geological Correlation Programme Project 516 (IGCP516) Geological Anatomy of East and South Asia, Kuala Lumpur, Malaysia.
- Shamseddin Meigoony, M., Afzal, P., Gholinejad, M., Yasrebi, A.B., Sadeghi, B., 2014. Delineation of geochemical anomalies using factor analysis and multifractal modeling based on stream sediments data in Sarajeh 1:100,000 sheet, Central Iran. *Arabian Journal of Geosciences*, 7: 5333–5343.
- Shi, J., Wang, C., 1998. Fractal analysis of gold deposits in China: implication for giant deposit exploration. *Earth Sciences Journal of China University Geosciences* 23: 616–618.
- Soltani, F., Moarefvand, P., Alinia, F., Afzal, P., 2019. Characterizing Rare Earth Elements by coupling multivariate analysis, factor analysis and geostatistical simulation; case-study of Gazestan deposit, central Iran. *Journal of Mining and Environment* 10: 929–945.
- Spalla, M.I., Morotta, A.M., Gosso, G., 2010. Advances in interpretation of geological processes: refinement of multi-scale data and integration in numerical modelling. Geological Society, London, 240 p.
- Sudi–Ajirlu, M., Jahangiri, A., 2010. Petrography and tectonic setting of Allahyarlu ophiolite. 21st Congress of Geological Sciences, Geological Survey of Iran (In Persian).
- Sudi–Ajirlu, M., Jahangiri, A., Moayyed, M., 2010. Relative dating of Allahyarlu ophiolite emplacement based on dating of limestones in core of Allahyarlu anticline, NW Iran. 5th Iranian Congress of Paleontology, Environmental Science Research Center, Kerman (In Persian).
- Turcotte, D.L., 1997. *Fractals and chaos in geology and geophysics*. Cambridge University Press, Cambridge, 1–398 pp.
- Wang, Q.F., Deng, J., Wan, L., Zhao, J., Gong, Q.J., Yang, L.Q., Zhou, L., Zhang, Z.J., 2008. Multifractal analysis of the element distribution in skarn–type deposits in Shizishan Orefield in Tongling area, Anhui province, China. *Journal of Acta Geologica Sinica*, 82: 896–905.
- Yasrebi, A.B., Hezarkhani, A., 2019. Resources classification using fractal modelling in Eastern Kahang Cu–Mo porphyry deposit, Central Iran. *Iranian Journal of Earth Sciences*, 11: 56–67.
- Yousefi M., Kamkar–Rouhani A., Carranza, E.J.M., 2012. Geochemical mineralization probability index (GMPI): a new approach to generate enhanced stream sediment geochemical evidential map for increasing probability of success in mineral potential mapping. *Journal of Geochemical Exploration*, 115: 24–35.
- Zamyad, M., Afzal, P., Pourkermani, M., Nouri, R., Jafari, M.R., 2019. Determination of Hydrothermal Alteration Zones by Remote Sensing Methods in Tirka Area, Toroud, NE Iran. *Journal of the Indian Society of Remote Sensing* 47: 1817–1830.
- Zuo, R., 2011a. Identifying geochemical anomalies associated with Cu and Pb–Zn skarn mineralization using principal component analysis and spectrum–area fractal modeling in the Gangdese Belt, Tibet (China). *Journal of Geochemical Exploration*, 111: 13–22.
- Zuo, R., 2011b. Decomposing of mixed pattern of arsenic using fractal model in Gangdese belt, Tibet, China. *Applied Geochemistry*, 26: S271–S273.
- Zuo, R., 2014. Identification of geochemical anomalies associated with mineralization in the Fanshan district, Fujian, China. *Journal of Geochemical Exploration*, 139: 170–176.
- Zuo, R., Agterberg, F.P., Cheng, Q., Yao, L., 2009. Fractal characterization of the spatial distribution of geological point processes. *International Journal of Applied Earth Observation and Geoinformation*, 11(6): 394–402.
- Zuo, R., Wang, J., 2016. Fractal/multifractal modeling of geochemical data: A review. *Journal of Geochemical Exploration*, 164: 33–41.
- Zuo, R., Xia, Q., Wang, H., 2013a. Compositional data analysis in the study of integrated geochemical anomalies associated with mineralization. *Applied Geochemistry*, 28: 202–211.
- Zuo, R., Xia, Q., Zhang, D., 2013b. A comparison study of the C–A and S–A models with singularity analysis to identify geochemical anomalies in covered areas. *Applied Geochemistry*, 33: 165–172.